# A general method for improving spatial resolution by optimization of electron multiplication in CCD imaging

**Pei-Hsun Wu,[1,2] Nathaniel Nelson,[1] and Yiider Tseng[1,2]***

[1]*Department of Chemical Engineering, Museum Road, University of Florida, Gainesville, Florida 32611, USA*

[2]*National Cancer Institute-Physical Science Oncology Center, Chemical Engineering Building, Museum Road, Gainesville, FL 32611, USA*

**ytseng@che.ufl.edu*

**Abstract:** The electron-multiplying charge-coupled device (EMCCD) camera possesses an electron multiplying function that can effectively convert the weak incident photon signal to amplified electron output, thereby greatly enhancing the contrast of the acquired images. This device has become a popular photon detector in single-cell biophysical assays to enhance subcellular images. However, the quantitative relationship between the resolution in such measurements and the electron multiplication setting in the EMCCD camera is not well-understood. We therefore developed a method to characterize the exact dependence of the signal-to-noise-ratio (*SNR*) on EM gain settings over a full range of incident light intensity. This information was further used to evaluate the EMCCD performance in subcellular particle tracking. We conclude that there are optimal EM gain settings for achieving the best *SNR* and the best spatial resolution in these experiments. If it is not used optimally, electron multiplication can decrease the *SNR* and increases spatial error.



**OCIS codes:** (040.0040) Detectors; (040.1520) CCD, charge-coupled device; (100.0100) Image processing; (100.2000) Digital image processing; (100.2960) Image analysis; (110.2970) Image detection systems; (110.3000) Image quality assessment; (170.2520) Fluorescence microscopy; (170.1530) Cell analysis; (330.6130) Spatial resolution.

## References and links

1. C. H. Eskiw, G. Dellaire, J. S. Mymryk, and D. P. Bazett-Jones, "Size, position and dynamic behavior of PML nuclear bodies following cell stress as a paradigm for supramolecular trafficking and assembly," J. Cell Sci. **116**(21), 4455–4466 (2003).
2. A. A. Gerencser, J. Doczi, B. Töröcsik, E. Bossy-Wetzel, and V. Adam-Vizi, "Mitochondrial swelling measurement in situ by optimized spatial filtering: astrocyte-neuron differences," Biophys. J. **95**(5), 2583–2598 (2008).
3. S. M. Görisch, M. Wachsmuth, C. Ittrich, C. P. Bacher, K. Rippe, and P. Lichter, "Nuclear body movement is determined by chromatin accessibility and dynamics," Proc. Natl. Acad. Sci. U.S.A. **101**(36), 13221–13226 (2004).
4. E. S. Levitan, F. Lanni, and D. Shakiryanova, "In vivo imaging of vesicle motion and release at the Drosophila neuromuscular junction," Nat. Protoc. **2**(5), 1117–1125 (2007).
5. C. Bakal, J. Aach, G. Church, and N. Perrimon, "Quantitative morphological signatures define local signaling networks regulating cell morphology," Science **316**(5832), 1753–1756 (2007).
6. M. Benoit, D. Gabriel, G. Gerisch, and H. E. Gaub, "Discrete interactions in cell adhesion measured by single-molecule force spectroscopy," Nat. Cell Biol. **2**(6), 313–317 (2000).
7. T. P. Kole, Y. Tseng, L. Huang, J. L. Katz, and D. Wirtz, "Rho kinase regulates the intracellular micromechanical response of adherent cells to rho activation," Mol. Biol. Cell **15**(7), 3475–3484 (2004).
8. G. Fink, L. Hajdo, K. J. Skowronek, C. Reuther, A. A. Kasprzak, and S. Diez, "The mitotic kinesin-14 Ncd drives directional microtubule-microtubule sliding," Nat. Cell Biol. **11**(6), 717–723 (2009).

#118505 - $15.00 USD Received 13 Oct 2009; revised 22 Jan 2010; accepted 6 Feb 2010; published 26 Feb 2010

9. J. Y. Xu, Y. Tseng, C. J. Carriere, and D. Wirtz, "Microheterogeneity and microrheology of wheat gliadin suspensions studied by multiple-particle tracking," Biomacromolecules **3**(1), 92–99 (2002).
10. I. McWhirter, "Electron Multiplying CCDs - New Technology for Low Light Level Imaging," Proceedings of 33rd annual European meeting on atmospheric studies by optical methods IRF science report **292**, 61–66 (2008).
11. M. Jonas, H. Huang, R. D. Kamm, and P. T. So, "Fast fluorescence laser tracking microrheometry. I: instrument development," Biophys. J. **94**(4), 1459–1469 (2008).
12. Y. Chen, J. D. Müller, P. T. So, and E. Gratton, "The photon counting histogram in fluorescence fluctuation spectroscopy," Biophys. J. **77**(1), 553–567 (1999).
13. A. Yildiz, M. Tomishige, R. D. Vale, and P. R. Selvin, "Kinesin walks hand-over-hand," Science **303**(5658), 676–678 (2004).
14. J. R. Unruh, and E. Gratton, "Analysis of molecular concentration and brightness from fluorescence fluctuation data with an electron multiplied CCD camera," Biophys. J. **95**(11), 5385–5398 (2008).
15. J. Hynecek, "Impactron-a new solid state image intensifier," IEEE Trans. Electron. Dev. **48**(10), 2238–2241 (2001).
16. L. Zhang, L. Neves, J. S. Lundeen, and I. A. Walmsley, "A Characterization of the Single-photon Sensitivity of an Electron Multiplying Charge-Coupled Device," J. Phys. B **42**(11), 114011 (2009).
17. M. S. Robbins, and B. J. Hadwen, "The noise performance of electron multiplying charge-coupled devices," IEEE Trans. Electron. Dev. **50**(5), 1227–1232 (2003).
18. S. Li, S. L. Lian, J. J. Moser, M. L. Fritzler, M. J. Fritzler, M. Satoh, and E. K. Chan, "Identification of GW182 and its novel isoform TNGW1 as translational repressors in Ago2-mediated silencing," J. Cell Sci. **121**(24), 4134–4144 (2008).
19. P. H. Wu, S. H. Arce, P. R. Burney, and Y. Tseng, "A novel approach to high accuracy of video-based microrheology," Biophys. J. **96**(12), 5103–5111 (2009).
20. T. Savin, and P. S. Doyle, "Static and dynamic errors in particle tracking microrheology," Biophys. J. **88**(1), 623–638 (2005).
21. R. C. Gonzalez, and R. E. Woods, *Digital Image Processing* (Prentice Hall, Upper Saddle River, NJ, 2002).
22. Y. Reibel, M. Jung, M. Bouhifd, B. Cunin, and C. Draman, "CCD or CMOS Camera Noise Characterisation," Eur. Phys. J. D **21**, 75–80 (2003).
23. J. C. Mullikin, L. J. van Vliet, H. Netten, F. R. Boddeke, G. van der Feltz, and I. T. Young, "Methods For CCD Camera Characterization," SPIE Image Acquis. Sci. Imaging Syst. **2173**, 73–84 (1994).
24. S. Weidtkamp-Peters, T. Lenser, D. Negorev, N. Gerstner, T. G. Hofmann, G. Schwanitz, C. Hoischen, G. Maul, P. Dittrich, and P. Hemmerich, "Dynamics of component exchange at PML nuclear bodies," J. Cell Sci. **121**(16), 2731–2743 (2008).
25. B. Kannan, L. Guo, T. Sudhaharan, S. Ahmed, I. Maruyama, and T. Wohland, "Spatially resolved total internal reflection fluorescence correlation microscopy using an electron multiplying charge-coupled device camera," Anal. Chem. **79**(12), 4463–4470 (2007).

## 1. Introduction

Single-cell biophysical assays that quantify size [1], morphology [2] and movement [3,4] of subcellular components can provide great insight into macromolecular function and effectively bridge the biological activities at the cellular and the molecular scale together [5]. However, given the heterogeneous nature of the cell structure, single cell measurements need to be performed with high resolution to produce accurate and statistically meaningful data [6,7]. The most straightforward way to conduct such measurements is through the analysis of individual images or a stack of images acquired with high-resolution microscopy [5,8,9]. Therefore, the success of these types of measurements relies on the capability of the camera to obtain high quality cell images. In modern microscopic systems, the most common device adopted as a photon detector is the charge-coupled device (CCD) camera, which can simultaneously use more than one million parallel arrays to sense the intensity profile of light emitted from objects within the visual field of the microscope. With this device, cell images with detailed information can be captured and later analyzed.

Yet, the performance of the CCD camera deteriorates with decreasing light intensity from the sample [10], and this significantly reduces the accuracy of low intensity subcellular measurements, such as in single molecule fluorescence imaging. This problem can be solved by acquiring images on much more expensive avalanche photodiode detectors (APD) or photomultiplier tubes (PMT) [11,12]. These types of detectors do not have large numbers of individual sensing units like the parallel array of the CCD camera. When acquiring information from the visual field of the microscope, an APD or a PMT sensor needs to use a scanning mode, which is usually much slower than the CCD camera. Therefore, if the spatial

#118505 - $15.00 USD Received 13 Oct 2009; revised 22 Jan 2010; accepted 6 Feb 2010; published 26 Feb 2010

resolution of low intensity images in a CCD camera can be improved, the CCD camera becomes the best choice due to its accessibility and high acquisition rate.

Several intensity-enhanced techniques have been developed to obtain high contrast images from low intensity signals such as intensified CCD (ICCD) and electron multiplying CCD (EMCCD) [10]. After the back-illuminated EMCCD camera was introduced, the sensitivity of EMCCD has outperformed the ICCD and the EMCCD has become a popular choice for imaging the dynamics of single molecules in cells [13,14]. EMCCD utilizes several specialized extended serial registers on the CCD chip to apply a high voltage and produce multiplying gain through the process of impact ionization in silicon [15]. This capability to elevate the photon-generated signal above the readout noise of the device even at high frame rates has made it possible to meet the need for ultra-low-light imaging applications without the use of external image intensifiers [16].

While the EMCCD camera is certainly promising for single particle tracking, a quantitative evaluation of the influence of EM gain on spatial resolution has not been performed. Therefore, we derived equations to relate the nominal EM gain with image intensity and the variance of image intensity. These equations were fit to experimental data to estimate the relevant image parameters. Quantitative mappings were used along with a Monte Carlo procedure to calculate the dependence of signal to noise ratio (*SNR*) and spatial positioning error on EM gain. We successfully optimized the EMCCD performance to achieve the best spatial resolution and *SNR* for particle tracking by this approach. Through this specific example, we have created a general method, applicable to other types of CCD cameras, which can optimize electron multiplication for subcellular imaging, and provide a quantitative guideline to improve the accuracy of subcellular biophysical assays.

## 2. Methods and results

### *2.1 The EM gain can influence quantitative image analysis*

EM gain is an analog signal multiplication feature that multiplies an electronic signal by applying high voltage across several CCD registers before readout [15]. The EM gain setting of the EMCCD camera aims to improve the contrast of the image. Image analysis uses intensity profiles of a group of specific pixels that describe an object. The intensity relations between the adjacent pixels are important for reliable tracking of a single particle. However, the EM gain function does not amplify the *SNR* equally for objects with different intensities [17]. In a typical particle tracking experiment, there are several objects of interest within the visual field, each with their own respective intensity profile designated by a group of pixels. If the EM gain setting does not evenly amplify all of these signals, then there may be an optimal EM gain setting for achieving the best spatial resolution.

To investigate this in more detail, two types of cellular bodies were probed to determine if the EM gain could preserve or consistently improve the spatial resolution of positioning. Cytoplasmic mRNA processing bodies (also called P-bodies or GW-bodies), labeled by GFP-Ago2 [18] through transfection, and nuclear promyelocytic leukemia (PML) bodies, labeled by YFP-Sumo1 (Addgene Inc., Cambridge, MA), were video-tracked without EM gain or with EM gain = 2000 in a fixed NIH 3T3 fibroblast using a TE 2000 microscope (Nikon, Melville, NY), equipped with a Cascade:1K EMCCD camera (Roper Scientific, Tucson, AZ) and a NA 1.45, oil-immersion 60 × objective lens (Nikon). For a specific type of EMCCD camera, the EM gain is an arbitrary number correlated to the applied voltage on the CCD registers. The range for our camera EM gain setting is between 0 and 4095. Through proper assignment of the region of interest (ROI) a high temporal resolution (30 Hz) can be achieved. In our case, the binning feature in the CCD camera is set as 3 × 3, resulting in a pixel size of 390 nm. Under these two EM settings, 300 experimental images repeatedly acquired from the same sample were used to assess the variance of positioning via particle tracking [19]. In brief, the raw images were subjected to a Gaussian kernel filter [20,21] to

#118505 - $15.00 USD Received 13 Oct 2009; revised 22 Jan 2010; accepted 6 Feb 2010; published 26 Feb 2010

reduce background noise before being fed into the 2D-particle tracking algorithm. The algorithm determined the particles' positions by least-square fitting their logarithmic intensities in the 3 × 3 binning area directly into a Gaussian curve:

$$\log I_P(x, y) = \log(I') - \frac{(x-\mu'_x)^2 + (y-\mu'_y)^2}{2\times R'^2_a}, \quad (1)$$

where the fitted peak intensity determines the particle's sub-pixel position, ( $\mu'_x$ , $\mu'_y$ ), within the central pixel of the binning area (the origin, (0, 0), is set to the center of the pixel). In Eq. (1), $I_P$ represents the pixel intensity of a particle and the fitted parameters, $I'$ , $R'_a$ , $\mu'_x$ , and $\mu'_y$ represent the particle's peak intensity, apparent radius, and the position in the x- and y-direction of a Cartesian plane, respectively. These results indicate that the positioning error strongly depends on the EM gain setting in a manner that depended on the intensity of the tracked object. (Fig. 1). Choosing an EM gain of 2000 increased the positioning error by as much as 48% (subcellular body #6) and decreased it by 44% (subcellular body #3).

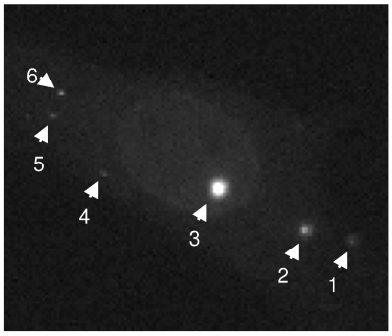


| Obj | positioning resolution (μm²) | | ratio |
|---|---|---|---|
| | $k = 0$ | $k = 2000$ | |
| 1 | $3.01\times10^{-3}$ | $2.31\times10^{-3}$ | 1.30 |
| 2 | $5.02\times10^{-4}$ | $5.04\times10^{-5}$ | 1.00 |
| 3 | $9.77\times10^{-5}$ | $1.74\times10^{-4}$ | 0.56 |
| 4 | $1.12\times10^{-2}$ | $1.36\times10^{-2}$ | 0.83 |
| 5 | $5.35\times10^{-3}$ | $3.72\times10^{-3}$ | 1.44 |
| 6 | $1.68\times10^{-3}$ | $1.14\times10^{-3}$ | 1.48 |

Fig. 1. EM gain causes contradictory effects on the spatial resolution of protein clusters. An NIH 3T3 fibroblast expressed two different proteins, GFP-Ago2 and YFP-Sumo1, forming two types of protein complexes containing one kind of fusion protein each. These speckle-like complexes (n = 6) were tracked to analyze the positioning error after the cell was fixed by formaldehyde. The analyzed results are listed in the table beside the image with the object numbers designated in the image. The effects of EM gain (at $k$ = 2000) on the resolution (presented by the variance of tracked positions) was listed as the ratio of the positioning resolution at $k$ = 0 to $k$ = 2000 (far right column).

*2.2 EM gain characterization*

The above result suggested that an optimal EM gain setting might exist to achieve the minimal positioning error in particle tracking. Thus, we developed a method to characterize the EM gain performance in the image acquisition process as it relates to subcellular particle tracking. Previously, we established a method to estimate the positioning error of particle tracking in an acquired image by direct mapping of the important image parameters using a Monte Carlo simulation technique. This method requires the information of a pixel's *SNR* profile over the whole intensity range. We derived the quantitative mapping between the intensity-dependent *SNR* and the EM gain as discussed below. This discussion will define many variables that are summarized in Table 1 for reference.

#118505 - $15.00 USD Received 13 Oct 2009; revised 22 Jan 2010; accepted 6 Feb 2010; published 26 Feb 2010

**Table 1. Summary of Notation**

| Notation (unit) | Description | Notation (unit) | Description |
|---|---|---|---|
| $I_P$ (au) | Pixel intensity of a particle | $I'$ (au) | Fitted particle's peak intensity |
| $R'_a$ (px) | Fitted particle's apparent radius | $\mu'_x$ (px) | Fitted particle's position in x-direction |
| $\mu'_y$ (px) | Fitted particle's position in y-direction | $N_P$ (photon) | Average number of incident photons per pixel on the CCD camera |
| $N_{PE}$ ($e^-$) | NP photons give rise to photo-activated electrons | $N_{DE}$ ($e^-$) | Dark current electrons |
| $k$ (-) | EM setting parameter for image acquisition | $G_{EM,k}$ (-) | Electron multiplication gain at EM setting $k$ |
| $G_{ADC}$ (au/$e^-$) | Analog to digital converter gain | $\sigma^2_{PS}$ ($e^{-2}$) | Photon shot noise |
| $I_{offset,k}$ (au) | Pixel intensity offset value at EM setting $k$ | $I_{out,k}$ (au) | Average output digital intensity per pixel at EM setting $k$ |
| $F_k$ (-) | Excess factor | $\sigma^2_R$ ($au^2$) | Read-out noise |
| $\sigma^2_{out,k}$ ($au^2$) | Total pixel intensity variance | $\varepsilon_{S,k}$ ($px^2$) | Spatial resolution in particle tracking |
| $SNR$ (-) | Signal to noise ratio | $I_{peak}$ (au) | Peak intensity of Gaussian particle at $k = 0$ |
| $I_{C,k}$ (au) | Critical $I_{peak}$ value at EM setting $k$ | $I_{BG}$ (au) | Background intensity |
| $R_a$ (px) | Gaussian particle size | | |

The derivation accounted for the conversion of incident photons into final pixel intensity (Fig. 2A). Consider $N_P$ as the average number of photons per pixel that are incident on the CCD camera coming from the observed object. $N_P$ photons give rise to $N_{PE}$ electrons. In addition, $N_{DE}$ electrons, dark current, are generated over time by thermal energy within the CCD camera, which are independent of the incident light on the detector [22]. Next, a fixed value of EM gain, $k$, which depends on the applied voltage [15], amplifies the electrons by a multiplication factor, $G_{EM,k}$. This multiplied electron signal is ultimately sent to the analog-digital converter that converts electron signals to an intensity count by a factor, $G_{ADC}$, with an offset, $I_{offset,k}$, to give the final average digital intensity per pixel, $I_{out,k}$. The described signal processing in an EMCCD camera can be mathematically represented as:

$$I_{out,k} = (N_{PE} + N_{DE}) \times G_{EM,k} \times G_{ADC} + I_{offset,k}. \quad (2)$$

Because the magnitude of dark current electrons increases with the exposure time [23], the effect of dark current electrons can be mitigated by decreasing the exposure time of the analyzed image. However, as seen in Eq. (2), the signal from dark current is multiplied by the effective EM gain, $G_{EM,k}$; hence, its effect on the magnitude of the output cannot be omitted at high $k$. Since the $I_{offset,k}$ value does not change with the binning setting of the CCD camera, which can boost the dark current signal depending on the integrated pixels, we adjusted the level of binning without incident light and used linear fitting to obtain the $I_{offset,k}$ in Eq. (2).

#118505 - $15.00 USD Received 13 Oct 2009; revised 22 Jan 2010; accepted 6 Feb 2010; published 26 Feb 2010

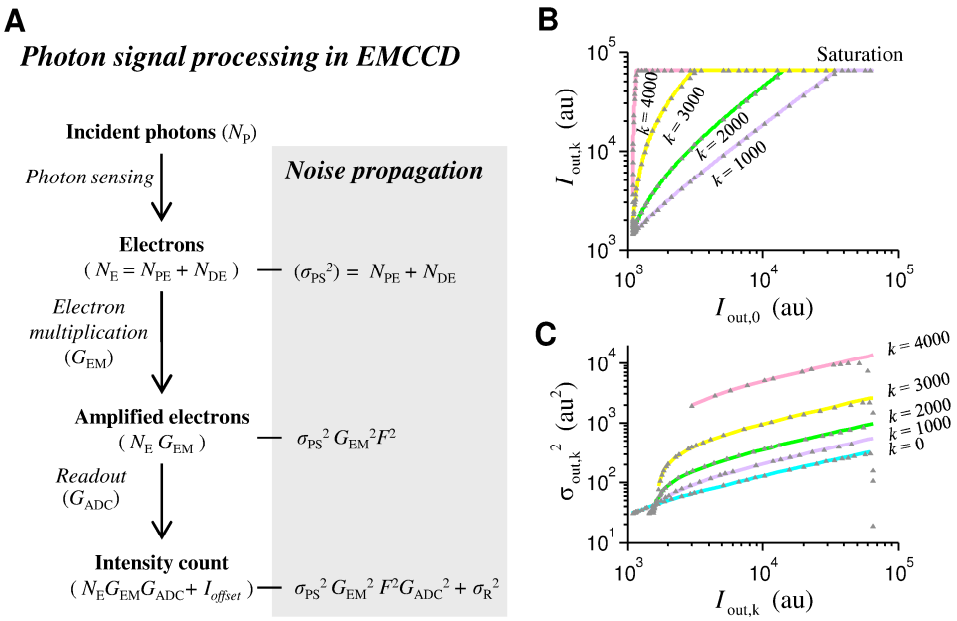


Fig. 2. EM gain parameters are determined experimentally. A. Schematic plot of photon conversion and noise propagation in the EMCCD camera. B. Logarithmic plot of intensity count ( $I_{out,k}$ ) at different EM gain (▲) versus $I_{out,0}$ under varying light intensities. The solid line represents the least squared fitting results to the linear model. Actual electron multiplication gain can be estimated from the slope of fitted model. **C.** Scatter plot of $\sigma_{out,k}^2$ versus $I_{out,k}$ at $k$ = 0, 1000, 2000, 3000 and 4000 in the logarithmic scale. Linear model fitting results at different EM gain are shown as a solid line and agree well with experimental data. $R^2 > 0.99$ for all fitted models.

At ground state ($k = 0$), Eq. (2) can be rearranged as:

$$(N_{PE} + N_{DE}) = (I_{out,0} - I_{offset,0}) / (G_{EM,0} \times G_{ADC}). \quad (3)$$

Substituting Eq. (3) into Eq. (2) with $G_{EM,0} = 1$, we get the following relation between the output intensity under electron multiplication ( $I_{out,k}$ ) and that in the ground state ( $I_{out,0}$ ):

$$I_{out,k} = G_{EM,k} \times I_{out,0} + I_{offset,k} - G_{EM,k} \times I_{offset,0}. \quad (4)$$

We acquired images at varying light source intensities at a fixed $k$, and measured average $I_{out,k}$ per pixel (for 100,000 pixels) corresponding to the different light intensities. These experiments were repeated for identical light source intensities at $k$ = 0. This resulted in a series of data points ( $I_{out,0}$ , $I_{out,k}$ ) corresponding to different light source intensities that were plotted for $k$ values varying from 1000 to 4000 (Fig. 2B). As seen in Fig. 2B, the $I_{out,k}$ saturates at high light source intensities. Since Eq. (4) only represents the relation between $I_{out,0}$ and $I_{out,k}$ before $I_{out,k}$ becomes saturated, we used this equation to fit unsaturated data points, which fit the data smoothly. Thus, the values of $G_{EM,k}$ were estimated at different values of $k$ and tabulated in Table 2. Notably, the relationship between the effective gain $G_{EM,k}$ and $k$ is not linear based on these trends.

#118505 - $15.00 USD Received 13 Oct 2009; revised 22 Jan 2010; accepted 6 Feb 2010; published 26 Feb 2010

**Table 2. The values of the effective EM gain ($k$), excess factor ($F$), intensity offset ($I_{offset}$), and relative working range at several EM gain settings estimated for our system.**

| $k$ | Effective EM gain ($G_{EM}$) | Excess factor ($F$) | $I_{offset}$ (au) | Relative working range to zero EM gain (%) |
|---|---|---|---|---|
| 0 | 1.00 | 1.00 | 1095.2 | 100.0 |
| 200 | 1.31 | 1.14 | 1383.1 | 75.9 |
| 500 | 1.47 | 1.17 | 1406.8 | 67.7 |
| 1000 | 1.90 | 1.24 | 1450.0 | 52.4 |
| 1500 | 2.80 | 1.29 | 1499.4 | 35.5 |
| 2000 | 4.98 | 1.34 | 1551.4 | 19.9 |
| 3000 | 33.41 | 1.41 | 1693.6 | 3.0 |
| 4000 | 878.82 | 1.38 | 2998.1 | 0.1 |

We next derived a quantitative relation between the variance in the measured intensity $I_{out,k}$ and effective EM gain $G_{EM}$. To do this, we accounted for noise propagation in the conversion process of $N_P$ photons to the variance in the final $I_{out,k}$. First, photon shot noise and dark current noise occur when photons are detected in each pixel, and their variances are equal to the signal magnitude [22]. This variance is given by $\sigma_{PS}^2 = \mathrm{var}(N_{PE} + N_{DE}) = N_{PE} + N_{DE}$. Electron multiplication further increases the variance by $G_{EM,k}^2$. In addition, the EM amplification process introduces an accumulated variance ($F_k^2$; where $F_k$ is called the excess factor) into the signal, which is generated from all the register steps [15]. Finally, the analog to digital converter converts the electronic signal to an output intensity count by the multiplication factor, $G_{ADC}$, also generating an additional signal independent read-out variance, $\sigma_R^2$. This leaves a total pixel intensity variance, $\sigma_{out,k}^2$, described by:

$$\sigma_{out,k}^2 = (N_{PE} + N_{DE}) \times G_{EM,k}^2 \times G_{ADC}^2 \times F_k^2 + \sigma_R^2. \quad (5)$$

Substituting the intensity count for the electronic signal, we get:

$$\sigma_{out,k}^2 = I_{out,k} \times G_{EM,k} \times G_{ADC} \times F_k^2 + \sigma_R^2 - I_{offset,k} \times G_{EM,k} \times G_{ADC} \times F_k^2. \quad (6)$$

In the above equation, the value of $G_{EM,k}$ is already known from the previous measurements and fitting. We next measured $\sigma_{out,k}^2$ as half of the variance of the pixel intensities in the image obtained from two repeated image subtractions (we accounted first for pattern noise, which is systematic variation in pixel intensities). Equation (6) was fit to the measured values of $\sigma_{out,k}^2$ and $I_{out,k}$ at $k$ = 0 where $F_0$ = 1; this allowed for the estimation of $G_{ADC}$ as 1.75 au per electron. This value was not expected to change as a function of $k$; therefore, we assumed this to be constant for fitting Eq. (6) to the data at non-zero values of $k$ (Fig. 2C). This allowed us to estimate the excess factor $F_k$.

In the high intensity region, the variance obtained by experiments was smaller than that of the theoretically estimated value. This is presumably a result of image saturation. The theoretical calculation does not take the saturation into account; hence, the estimated variance can represent the total shot noise and readout noise at high incident photon levels. In a real case, a signal with intensity higher than the maximum pixel output can cause the pixel to only export that maximum output value, giving rise to a signal loss. Thus, the mean and variance

#118505 - $15.00 USD Received 13 Oct 2009; revised 22 Jan 2010; accepted 6 Feb 2010; published 26 Feb 2010

of the output intensity count will be underestimated as the intensity count approaches saturation.

*2.3 The signal to noise ratio (SNR) can be used to optimize the EM gain setting*

One can also easily derive the *SNR* at various incident photon magnitudes as:

$$SNR = N_{PE} \times G_{EM,k} \times G_{ADC} \Big/ \sqrt{((N_{PE} + N_{DE}) \times G_{EM,k}^2 \times G_{ADC}^2 \times F_k^2 + \sigma_R^2)}. \quad (7)$$

With short acquisition times, the dark electron effect can be neglected. The $N_{PE}$ value can be calculated by Eq. (2) using the value of $I_{out,k}$. Therefore, we can estimate the theoretical *SNR* for different $N_{PE}$ at a given EM-setting from Eq. (7) since all parameters in this equation are known (Table 2). As a result, the theoretical *SNR* for $k$ = 2000 can be calculated over whole working range of light intensity. Meanwhile, this value can also be obtained from the value of $(I_{out,2000} - I_{offset,2000}) / \sigma_{out,2000}$, where $I_{out,2000}$ and $\sigma_{out,2000}$ can be measured experimentally. A comparison (Fig. 3A) shows that the experiments were in very good agreement with the theoretical estimates.

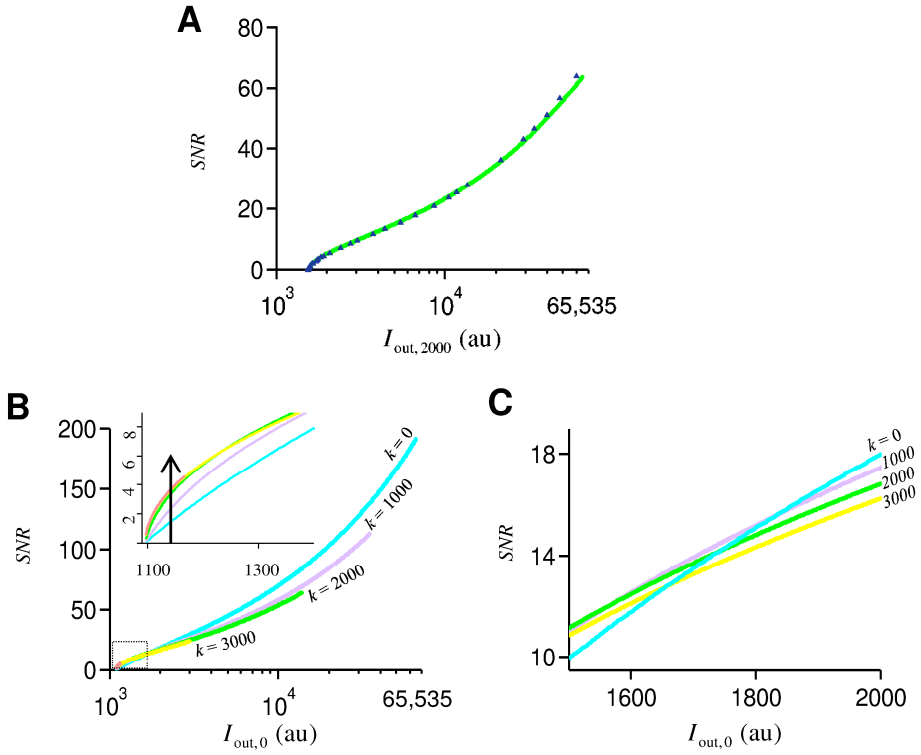


Fig. 3. The optimal setting of the EM gain depends on the intensity of the signal. A. The correlation between *SNR* and $I_{out,k}$ is plotted for $k$ = 2000. The theoretically derived *SNR* curve (solid line) agrees well with experimental data (▲). B. Values of the *SNR* at different EM gain ($k$ = 0, 1000, 2000, 3000 and 4000) are determined theoretically and plotted at the same amount of light intensity as $I_{out,0}$. At a high incident light intensity, the highest *SNR* is at $k$ = 0, and the *SNR* decreases with increasing $k$. *Inset*: the region marked by the dashed box in panel *B* is shown in more detail. The arrow points in the direction of increasing $k$. **C.** The *SNR* crossover between $k$ = 0 and a given $k$ occurs around $I_{out,0}$ = 1800 au.

#118505 - $15.00 USD Received 13 Oct 2009; revised 22 Jan 2010; accepted 6 Feb 2010; published 26 Feb 2010

This allowed us to estimate the *SNR* response for different EM gain settings from Eq. (7) at varying magnitudes of intensity. Comparison for the same amount of light intensity (i.e. $I_{out,0}$) but at different *k* values (Fig. 3B) indicates that changing the EM gain setting can result in different *SNR* values under identical illumination. At higher incident photon levels, *SNR* can be simplified to $\sqrt{N_{PE}} / F_k$ by neglecting the readout noise in Eq. (7). Hence, no single EM gain achieved the best performance as predicted by the minimization of the excess factor (Fig. 3B), but at lower $N_P$, increasing *k* enhances the *SNR* (Fig. 3B *inset*). The improvement of the *SNR* at low $N_P$ plateaus when *k* is above 2000 for our imaging system, and the *SNR* crossover takes place around $I_{out,0}$ = 1800 au (Fig. 3C).

### 3. EM gain effects on multi-pixel analysis

The above study revealed the capability of EM gain to improve the *SNR* at the single pixel level when the intensity of incident light is low, but that it has the opposite effect when the light intensity is high. The extent to which this can influence spatial resolution during particle tracking where multiple groups of pixels are analyzed is unclear. The different pixels may possess various intensities, and the EM process could introduce spatially varying error in the analysis. We therefore determined the effect of EM gain on the positioning error ($\varepsilon_S$; or spatial resolution) of particle positioning of a 100-nm particle using a Monte Carlo method published previously [19].

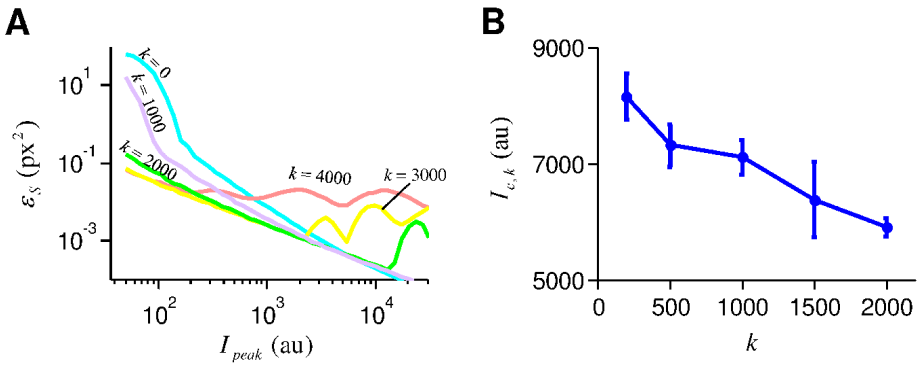


Fig. 4. The relation of the *k* and $\varepsilon_S$ is affected by $I_{peak}$. A. The EM gain setting affects the $\varepsilon_S$ dependency on $I_{peak}$. These results show that EM gain effectively improves the $\varepsilon_S$ at low signal intensity, but the effect diminishes with increasing $I_{peak}$ of the objects. After the $\varepsilon_S$ at a certain *k* crosses over that of *k* = 0 ($I_{peak}$ ~2000 au), a contrary effect occurs. B. The crossover points of the peak intensity at the junction of the positioning error curves of non-zero *k* and at *k* = 0 (●) depend on *k*. The crossover points set an upper bound as the critical points for the highest $I_{peak}$ values at a certain EM gain; at $I_{peak} < I_{C,k}$, one can still take the advantage of EM gain to reduce the positioning error in particle tracking experiments. The error bar is the standard deviation from five individual simulation results.

A Gaussian particle with a fixed radius was assigned different peak intensities sequentially to mimic real system conditions. Furthermore, proper magnitudes of random noise corresponding to the noise profile of the assigned signal intensity under the specified EM gain condition, were added to each pixel in the simulation [19]. Fixed pattern noise in our CCD camera has a minimal effect on particle resolution as demonstrated from Monte Carlo simulations (data not shown). Therefore, this type of noise was omitted from further simulations while identifying the $\varepsilon_S$ of a particle. The extracted $\varepsilon_S$ values correspond to

#118505 - $15.00 USD Received 13 Oct 2009; revised 22 Jan 2010; accepted 6 Feb 2010; published 26 Feb 2010

varying particle peak intensities ( $I_{peak}$ denotes the peak intensity at $k$ = 0, see Fig. 4A), showing that EM gain can significantly improve $\varepsilon_S$ by more than 10 fold when the $I_{peak}$ of the object is lower than 100 au. This EM gain effect decreases gradually and eventually reverses at high $I_{peak}$ (≥ 2000 au). For example, a Gaussian particle with $I_{peak}$ of 15,000 au possesses 2.3 times smaller $\varepsilon_S$ at $k$ = 0 than at $k$ = 2000. Saturation of a pixel can occur when the $I_{peak}$ of a Gaussian particle is high, and this caused a fluctuating and irregular correlation between $\varepsilon_S$ and $I_{peak}$ in the simulation results.

To understand the above phenomenon in more detail, we calculated the critical $I_{peak}$ value ( $I_{C,k}$ ), which is the intersection point of the $\varepsilon_S$ curves in Fig. 4A at $k$ = 0 and another EM gain setting $k$ (Fig. 4B). Due to the adverse effect of EM gain on $\varepsilon_S$ in object positioning at high intensity levels, the figure suggests a boundary (the $I_{C,k}$ – $k$ curve) to separate the regions between where EM gain activation is beneficial for object positioning and where it is not. The profile also sets a quantitative standard for applying adequate EM gain. It is important to note that increasing the EM gain reduces the working range of photon acquisition and therefore leads to a smaller working range of $I_{peak}$ values.

*3.1 Optimal EM gain depends on the size and background intensity of the object*

The above study suggests that the $I_{C,k}$ value depends on $k$ and can help determine whether EM gain should be applied to improve the resolution of a quantitative biophysical assay probing an object with known $I_{peak}$. To explore whether other physical parameters of the object also affect the $I_{C,k}$ value in particle tracking, the simulated Gaussian particle was used as an ideal and simplified model for mimicking cellular components. Different levels of background signal ( $I_{BG}$ ) were assigned to the simulation to examine how $I_{C,k}$ changes with $I_{BG}$. The results showed that an increase in $I_{BG}$ leads to a decrease in $I_{C,k}$ and when the $I_{BG}$ exceeds 900 au, both the $I_{C,1000}$ and $I_{C,2000}$ drop approximately to zero (Fig. 5A). Therefore, high background images reduce the advantage of EM gain activation.

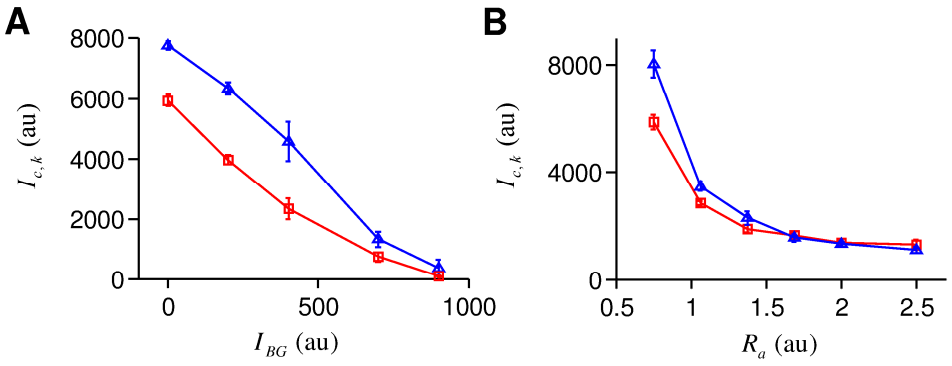


Fig. 5. The EM gain performance in particle tracking depends on experimental conditions. A. Background intensity, $I_{BG}$, affects the $I_{C,k}$ significantly. With $I_{BG}$ > ~900 au, the EM gain will not improve the $\varepsilon_S$ for particle tracking. B. A large apparent radius of particle, $R_a$, also affects the $I_{C,k}$ significantly. Open triangles (△) and open squares (□) correspond to $k$ = 1000 and 2000, respectively.

#118505 - $15.00 USD Received 13 Oct 2009; revised 22 Jan 2010; accepted 6 Feb 2010; published 26 Feb 2010

We next evaluated the effects of particle size and sub-pixel location on $I_{C,k}$. Gaussian particles with different sizes or sub-pixel locations were used again as a simplified model. The simulated results suggested that the $I_{C,1000}$ and $I_{C,2000}$ values drop quickly with increasing apparent radius of an object (Fig. 5B) but the sub-pixel location of the Gaussian bead does not have a significant effect on the $I_{C,1000}$ and $I_{C,2000}$ values (data not shown). In essence, these studies demonstrate that the EM gain is most effective in a biophysical assay such as particle tracking and positioning when the object possesses a small radius, low peak intensity, and low background intensity.

*3.2 Particle tracking experiments verify the EM gain effect on image analysis*

These simulation results were verified through the tracking of fixed 100-nm fluorescent microspheres. The $\varepsilon_{S,k}$, based on the positioning error in 600 trials of positioning a fixed microsphere, were determined at a fixed EM gain. An x - y diagram was used to describe the results (Fig. 6). The x-axis represents the $\varepsilon_{S,0}$, while the y-axis represents the $\varepsilon_{S,1000}$. In this case, the straight line, x = y, divides the diagram into two regions: above the line, there is a detrimental EM gain effect (i.e., $\varepsilon_S$ becomes larger when EM gain is activated) and below the line, there is a beneficial EM gain effect (i.e., $\varepsilon_S$ becomes smaller when the EM gain is activated). If the $\varepsilon_{S,k}$ value falls on the line, then it means that EM gain has no significant effect on the $\varepsilon_S$. Since the concentration of the microspheres can contribute to the $I_{BG}$, a sample with a high concentration of fixed, out-of-focus fluorescent microspheres was used to create a high $I_{BG}$, which was 2000 au higher than the dark current under the full power of the UV light source. Under such conditions, 35 in-focus particles were tracked (shown as hollow squares) to assess their $\varepsilon_{S,0}$ and $\varepsilon_{S,1000}$ values. In parallel, 43 fixed, fluorescent microspheres were tracked in samples with lower particle concentrations and lower excitation light intensity (shown as solid circles), which produced low $I_{BG}$ ( = 1200 au, which contains the intrinsic $I_{offset,k}$ value, see Eq. (2)) and low $I_{peak}$ (lower than 2000 au). Results obtained from these experiments confirmed that EM gain performance on the $\varepsilon_S$ of particle-tracking experiments depends on $I_{BG}$ and $I_{peak}$, and that EM gain can damage the resolution of experiments at higher $I_{BG}$.

#118505 - $15.00 USD Received 13 Oct 2009; revised 22 Jan 2010; accepted 6 Feb 2010; published 26 Feb 2010

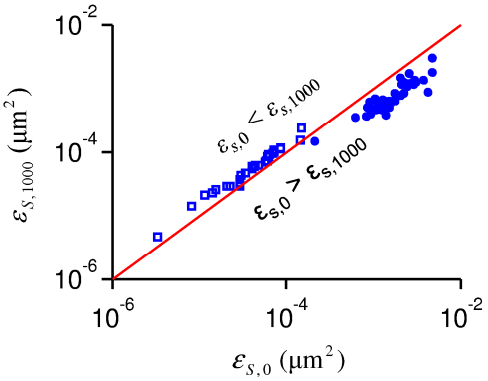


Fig. 6. Plot of $\varepsilon_{S,1000}$ vs. $\varepsilon_{S,0}$. Two experimental conditions were chosen: 35 microspheres at high $I_{peak}$ at 100% light source intensity (□) and 43 microspheres at low $I_{peak}$ at 25% power of light source intensity (●). The solid line corresponds to $\varepsilon_{S,1000} = \varepsilon_{S,0}$. Zero EM gain causes a 23% ( ± 10%) improvement in positioning error at 100% light source intensity in which $I_{peak}$ is larger than 10,000 au and background intensity is ~5000 au. On the other hand, EM gain ($k$ = 1000) improved the positioning error by 46% ( ± 11%) for the particle with small $I_{peak}$ (~1000 au) and minimal background ( $I_{BG}$ ~0 at 25% light source intensity).

## 4. Conclusion

The EM gain magnifies the photon-signal-induced electron flow in individual pixels of a CCD camera. A higher EM gain can generate more output from the pixel until the pixel reaches its maximum output capacity (saturation). This saturation sets the working range that should be used when amplifying the incident signal. A quantitative method to assess the outcome after using EM gain and evaluate its effectiveness in a biophysical assay is essential to ensure high resolution in subcellular measurements. Therefore, here we investigate EM gain effects on simulated Gaussian shaped particles to gain an understanding of the optimal EM gain settings in cellular particle tracking.

We adopt this model system for three purposes. First, particle tracking is a powerful technique in cellular biophysics. Information gained from this approach can have a direct and immediate impact on the particle tracking community. Second, a Gaussian shaped particle is relatively easy to evaluate. Hence, results obtained from this model can be more easily verified than other models. Last, the evaluation procedure developed by use of this model can be extended as a platform to explore the effectiveness of EM gain on biophysical studies of cellular components with more complicated features.

### *4.1 The working range and effectiveness of EM gain*

We previously presented that accuracy in particle-positioning relies heavily on a high *SNR* in acquired images [19]. Here, we further explored how the EM gain settings in a CCD camera can affect the *SNR* in acquired images. We modified an established method [22] to quantify the dependence of the *SNR* values on the EM gain, *k*, of an EMCCD camera and evaluated to which extent the EM gain could affect the outcome of a particle tracking experiment. After comparing the *SNR* values for different *k* values over a full range of incident light, we concluded that the EM gain only enhances the *SNR* of an output signal when the incident light intensity is lower than a certain critical level (in our case, it is 1900 au as measured at $k$ = 0). When the incident light intensity is higher than that critical level, it will diminish the *SNR* value and damage the fidelity of particle tracking results. We also concluded that the working

#118505 - $15.00 USD Received 13 Oct 2009; revised 22 Jan 2010; accepted 6 Feb 2010; published 26 Feb 2010

range of a particle tracking experiment is determined by the maximum $I_{peak}$ of a group of tracked particles because the electron multiplication of the brightest particle will more quickly result in saturation of the amplified maximum peak intensity ( $I_{out}$ ), reducing accuracy in particle positioning. The maximum $I_{peak}$ values allowed in our system are 12,840, 1,910 and 71 au (using $k$ = 0 as a reference) for $k$ = 2000, 3000 and 4000, respectively. This demonstrates that the working range for EM gain in particle tracking diminishes quickly with increasing EM gain when $k$ is larger than 2000.

Although the maximum pixel intensity allowed before saturation at $k$ = 2000 is over 10,000 au in our experimental system as suggested in data shown in Fig. 4A, our simulation results suggest that the smaller positioning error compared to that at $k$ = 0 for particle tracking occurs only when the $I_{peak} \leq 6000$ au. Hence, application of the highest $k$ allowed by the working range will not necessarily produce the most accurate tracking result. Presumably this is because particle tracking needs to quantitatively analyze the intensity profile over a group of pixels to identify the position or boundary information. Since the *SNR* of a pixel at different intensities does not linearly depend on the EM gain setting, the relative intensities among the group of pixels representing the object of interest are quantitatively altered, changing the outcome of their calculated positions.

*4.2 Analysis of the estimated values in this study*

In our evaluation, the extraction of the $G_{ADC}$ value plays a critical role to determine the excess factor, $F_k$ . The range of $G_{ADC}$ within a 95% confidence interval was found to be 0.028, representing 3.96 times of its standard deviation. The standard deviation of $G_{ADC}$ estimated from this information is 0.007, which is 0.4% of its mean value. This can be quickly verified by calculating the standard deviation for $G_{ADC}$ using four independent trials, which was found to be less than 0.8%. Therefore, using the extreme values of $G_{ADC}$ (2 standard deviations from the mean), we could estimate the range of excess factor, $F_k$ , which was found to be within 0.98 ~1.02 times its mean value, or approximately within 2% of the mean in all different conditions. From this analysis, we expect that other parameters that can be derived based on the extracted $G_{ADC}$ value will also possess very little deviation from their mean values.

*4.3 Assessment of EM gain in subcellular particle tracking experiments*

The signal is highly sensitive to the EM gain setting, and our results suggest that the EM gain is not very useful for tracking particles that are typically brightly visible and clearly defined in the image (such as YFP-sumo). Our imaging experiments provide an example to demonstrate this phenomenon. A PML-nuclear body labeled by YFP-sumo has high background intensity, presumably caused by the freely diffusive YFP-sumo molecules in the nucleus [24]. This nuclear body also has high intensity and large radius. Therefore, it is not beneficial to track YFP-sumo-labeled PML-nuclear bodies using an EM gain setting. In contrast, electron multiplication favored the tracking of GW-bodies with dimmer intensities and possessing smaller radii. This study provides direct evidence to demonstrate that the EM gain setting of the EMCCD camera can significantly influence the positioning error during subcellular particle tracking.

*4.4 Application of proper EM gain to biophysical measurements beyond particle tracking*

Many biophysical studies utilize signals generated from GFP or their derivatives. The applications of GFP in quantitative cellular biophysics are very powerful but are challenging at low intensities. If the GFP molecules emit light with low intensity, the acquired image

#118505 - $15.00 USD Received 13 Oct 2009; revised 22 Jan 2010; accepted 6 Feb 2010; published 26 Feb 2010

possesses a low *SNR* value and the accuracy of the biophysical assay is reduced. On the other hand, if the exposure time is increased, photo-bleaching effects become unavoidable. In most cases, it is best to minimize the UV-light exposure so a consistent signal output can be maintained. Therefore, a proper EM gain setting could greatly improve the accuracy of biophysical assays for low-intensity signals. Electron multiplication can effectively reduce the required image intensity and extend the possible experimental time frame without affecting spatial resolution. Under optimal EM gain settings, the pixel intensity can be more reliably measured for photon counting histogram analysis [12]. In this regard, the EMCCD camera can be used to improve the detection of molecular fluctuations in micro-scale volumes and improve the reliability of fluorescence correlation spectroscopy (FCS) [25] or concentration measurements [14]. In these types of studies, the EM gain feature is critical to successfully amplify the photon fluctuation to overcome readout noise since the photon count in the pixel is usually small.

In an effort to achieve the highest accuracy in microscopy-based biophysical measurements, a standard procedure to analyze the EM gain settings of a CCD camera is developed in this study. These quantitative cellular biophysical assays usually focus on imaging subcellular dynamics. Often, a quantitative measurement is required, and the accurate positioning of the subcellular object in image analysis becomes a critical step for the success of the biophysical assay. The parameters that can affect EM performance include the exposure time of image acquisition (temporal resolution), the background intensity and shape of the probed object. To be applicable to a broad range of experimental situations, this EMCCD characterization must be available for a variety of particle shapes, sizes and intensities. The method we have provided in this study is theoretically suitable for all types of EMCCD camera. Since the intensified CCD (ICCD) camera has similar signal amplification processing (photon signal is enhanced first in a similar way and sensed by CCD chip later) but a different physical mechanism; it is expected that some minor modifications to our method may be required to accurately assess the optimal settings for an ICCD camera. However, further verification is required. Nevertheless, this study provides a method to quantitatively choose the appropriate EM gain for maximizing the resolution of biophysical assays. The optimization procedure presented here should greatly improve the accuracy of such measurements.

**Acknowledgments**

The authors are grateful for Dr. Tanmay Lele and Mr. Stephen Hugo Arce for their thoughtful discussion. This research was partially funded by National Institutes of Health grants U54CA143868 and EB004416.

#118505 - $15.00 USD Received 13 Oct 2009; revised 22 Jan 2010; accepted 6 Feb 2010; published 26 Feb 2010